Magnetic critical behavior of fractals in dimensions between 2 and 3

Pai-Yi Hsiao,[1] Pascal Monceau,[1,2] and Michel Perreau[1]
[1]*Laboratoire de Physique Théorique de la Matière Condensée, Université Paris 7–Denis Diderot, case 7020, 2 place Jussieu, 75251 Paris Cedex 05, France*
[2]*Département de Physique et Modélisation, Université d'Evry-Val d'Essonne, Boulevard F. Mitterrand, 91025 Evry Cedex, France*
(Received 28 August 2000)

We report the critical exponent values of the Ising model, ν^{-1}, γ/ν, and β/ν, and the critical temperatures of three Sierpínski fractals with Hausdorff dimensions d_f equal to 2.966, 2.904, and 2.631. The results are calculated from finite-size scaling analysis by Monte Carlo simulations. They are precise enough to show that the hyperscaling relation $d_f=2\beta/\nu+\gamma/\nu$ is satisfied. Furthermore, the discrepancy between the values provided by ϵ expansions and by Monte Carlo simulations shows that the critical behavior of fractals cannot be fully understood in the framework of strong universality.

Fractal networks are natural candidates to interpolate between integer dimensions. Since they do not exhibit translation symmetry, but scale invariance, the question which must be considered in dealing with phase transitions in such systems is the following: How is the critical behavior affected by this replacement. The early works on phase transitions in fractal structures were done by Gefen *et al.*[1–4] They studied these systems with the help of real space renormalization group methods; they found that the Hausdorff dimension should replace the space dimension in the description of the critical phenomena. Later, Bhanot *et al.*[5,6] performed Monte Carlo simulations with the Metropolis algorithm and suggested that the average number of bonds per spin should be used instead of the Hausdorff dimension. Recently, magnetic phase transitions of the ferromagnetic Ising model on Sierpinski carpets have been studied by two groups, using powerful Monte Carlo simulation methods, mainly the Wolff algorithm able to reduce significantly the critical slowing down.[7,8] They explored a range between the lower critical dimension of the Ising model, $d=1$ and $d=2$. They both found that scaling corrections are strong, and interpreted this result as a consequence of the slow convergence of the thermal averages towards the infinite limit as the size of the lattice increases. Nevertheless, they were able to study large enough systems to show that the values of the critical exponents β/ν and γ/ν for two different fractal dimensions ($d_f=1.8927$ and $d_f=1.7925$) satisfy the hyperscaling law $d_f=2\beta/\nu+\gamma/\nu$; here, d_f is the Hausdorff dimension of the fractal. We are now able to study numerically the critical properties of the Ising model for fractal dimensions between $d=2$ and $d=3$. No precise simulation results were available, up to now, between two integer dimensions exhibiting a phase transition at nonzero temperature.

We will call the fractals we deal with ''Sierpínski sponges'' and denote them by the symbol SP(l^d,N_{occ},k) where l is the size of the generating cell, $d=3$ (the dimension of embedding space), N_{occ} is the number of occupied sites in the generating cell, and k is the number of iteration steps. The spins are located in the center of the occupied sites. The ''Sierpínski sponge'' is generated as follows: At the kth iteration step we enlarge the $(k-1)$th iteration lattice by replacing each occupied site by the whole generating cell; the size of the network generated after k steps is $L=l^k$. All information about the geometrical properties of a given fractal is determinated by this cell SP(l^d,N_{occ},$k=1$). The l sections of the generating cells associated with the three different fractals which we will study are shown in Fig. 1. The fractal in the mathematical sense is obtained only when k tends towards infinity and we call it SP(l^d,N_{occ}). Here SP(3^3,26) and SP(3^3,18) will be explored up to the fifth iteration step where $L=243$ and SP(4^3,56) to the fourth iteration step where $L=256$. These fractals have infinite rami-

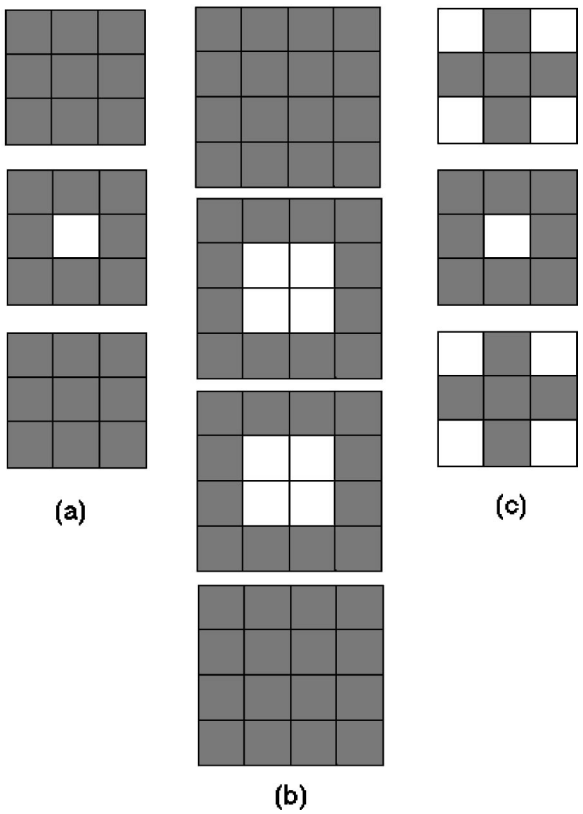

FIG. 1. The generating cell of Sierpínski sponges: (a) SP(3^3,26,1), (b) SP(4^3,56,1), and (c) SP(3^3,18,1). The pictures are shown section by section. Each shadowed square represents one spin-occupied site.

TABLE I. The maximum values of $\phi_L(T)$, $\chi_L(T)$, and $C_L(T)$ and the associated temperatures $T^{\phi}(L)$, $T^{\chi}(L)$, and $T^{C}(L)$ with respect to the different iteration steps k for the Sierpiński sponges. The values of ν^{-1}, γ/ν, and T_c are listed in the last column.

Fractal SP		$k=1$	$k=2$	$k=3$	$k=4$	$k=5$	$\nu^{-1}, \gamma/\nu, T_c$
(3^3,26)	$\phi_L^{\max}$	8.87(3)	53.5(3)	297.4(1.9)	1591(24)	8293(359)	$\nu^{-1}=1.503(53)$
	$T^{\phi}(L)$	4.826(5)	4.276(1)	4.2268(6)	4.2188(2)	4.2173(1)	$T_c=4.2170(2)$
	$\chi_L^{\max}$	0.4513(5)	4.58(1)	40.89(17)	350.3(2.5)	2963(38)	$\gamma/\nu=1.943(18)$
	$T^{\chi}(L)$	4.243(2)	4.2275(5)	4.2193(2)	4.21749(8)	4.21710(3)	$T_c=4.21701(6)$
	$C_L^{\max}$	0.950(1)	1.788(6)	2.50(2)	3.16(4)	3.8(1)	—
	$T^{C}(L)$	3.768(2)	4.108(2)	4.1947(9)	4.2127(3)	4.2163(1)	$T_c=4.2171(2)$
(4^3,56)	$\phi_L^{\max}$	13.10(2)	108.0(5)	800(14)	5646(181)	—	$\nu^{-1}=1.410(36)$
	$T^{\phi}(L)$	4.394(3)	4.038(1)	4.0046(4)	3.9997(1)	—	$T_c=3.99889(23)$
	$\chi_L^{\max}$	0.817(1)	13.43(4)	191.9(1.6)	2729(25)	—	$\gamma/\nu=1.915(13)$
	$T^{\chi}(L)$	4.098(1)	4.0169(6)	4.0019(2)	3.99935(6)	—	$T_c=3.99893(10)$
	$C_L^{\max}$	1.141(2)	1.972(8)	2.514(23)	2.97(10)	—	—
	$T^{C}(L)$	3.754(2)	3.9588(9)	3.9936(4)	3.9983(4)	—	$T_c=3.9991(6)$
(3^3,18)	$\phi_L^{\max}$	4.857(6)	19.63(6)	76.3(4)	287.5(4.0)	1058(16)	$\nu^{-1}=1.185(27)$
	$T^{\phi}(L)$	3.579(3)	2.578(2)	2.409(1)	2.3667(4)	2.3553(2)	$T_c=2.3510(4)$
	$\chi_L^{\max}$	0.5321(7)	5.53(2)	50.4(5)	451(1)	4020(21)	$\gamma/\nu=1.991(7)$
	$T^{\chi}(L)$	2.915(1)	2.5193(6)	2.3976(3)	2.36379(9)	2.35440(4)	$T_c=2.35090(9)$
	$C_L^{\max}$	0.810(1)	1.456(4)	1.85(3)	2.08(2)	2.21(2)	—
	$T^{C}(L)$	2.595(1)	2.427(2)	2.371(8)	2.3577(9)	2.3527(6)	$T_c=2.35089(12)$

fication order; it ensures that they exhibit a second-order phase transition at nonzero temperature.[4] For a given temperature T and a given size L, we call $\langle E_L\rangle_T$ and $\langle M_L\rangle_T$ the canonical thermal averages of the total energy and of the absolute value of the total magnetization, respectively. The specific heat per spin of the system reads $C_L(T)=(\langle E_L^2\rangle_T - \langle E_L\rangle_T^2)/(N_{occ}T^2)$. The thermal average of the absolute value of the magnetization per spin is $m_L(T)$ and the zero-field magnetic susceptibility per spin is $\chi_L(T)=(\langle M_L^2\rangle_T - \langle M_L\rangle_T^2)/(N_{occ}T)$. The logarithmic derivative of the magnetization is defined as $\phi_L(T)=\partial \ln\langle M_L\rangle_T/\partial\beta_B$ where β_B is the inverse of temperature. According to Fisher's finite-size scaling theory,[9] the exponents ν^{-1}, γ/ν, and α/ν can be extracted from the slopes of the fitting lines in log-log plots of the size L versus the maximum values of $\phi_L(T)$, $\chi_L(T)$, and $C_L(T)$, respectively. The critical temperature T_c for the infinite system can be hence estimated from the positions of the peaks $T^{\kappa}(L)$ ($\kappa=\phi$, χ, or C) of $\phi_L(T)$, $\chi_L(T)$, and $C_L(T)$ according to the relation

$$T^{\kappa}(L)=T_c+g_{\kappa}L^{-1/\nu}, \tag{1}$$

where g_{κ}'s are physical quantity-dependent constants. Moreover, we can also find the exponents by performing simulations at the critical temperature because of the linear dependence of $\phi_L(T_c)$ on $L^{1/\nu}$, $C_L(T_c)$ on $L^{\alpha/\nu}$, $m_L(T_c)$ on $L^{-\beta/\nu}$, and $\chi_L(T_c)$ on $L^{\gamma/\nu}$.

We perform the high-efficient Wolff algorithm[10] to generate our spin configurations. Periodic boundary conditions are chosen in order to eliminate the surface free energy contribution.[11] For each iteration step k, at each simulation temperature T, we execute 10^6 Monte Carlo steps. The histogram method is then applied to extract all possible information near this simulation temperature. The reliable temperature range is carefully estimated for each thermal average. We repeat the whole above processes at least ten times to get a sufficient number of samples to perform statistical analysis of our data. All the error bars which we will give below are statistical standard deviations. In Table I, we give the maximum values of $\phi_L(T)$, $\chi_L(T)$, and $C_L(T)$ at each iteration step of the fractal structures. The temperatures where these peaks occur are listed just below them. The maxima of $\phi_L(T)$ and $\chi_L(T)$ associated with the last three iteration steps as a function of L nearly line up in log-log plots. In order to estimate properly the exponents ν^{-1} and γ/ν, we measure the slopes from the last two iteration steps, and compare them with that extracted from the last three steps: The differences observed are always smaller than 3%. The critical temperatures for the infinite systems can be then obtained from Eq. (1) provided that ν^{-1} is known. The results are given in the last column of Table I. For each studied fractal SP(l^d,N_{occ}) the values of T_c obtained from the positions of the peaks of $\phi_L(T)$, $\chi_L(T)$, and $C_L(T)$ are consistent, within the accuracy of the simulations. Nevertheless, the maxima of the specific heat $C_L(T)$ do not follow a power law up to the iteration steps that we have done. It is the reason why we cannot give the corresponding exponent values α/ν in Table I.

We are now able to turn our attention to the critical behavior at T_c. The most precise values of T_c are estimated from the positions of the peaks of $\chi_L(T)$ and lead to 4.217 01, 3.998 93, and 2.350 90 for SP(3^3,26), SP(4^3,56), and SP(3^3,18), respectively. These values are consistent, within the error bars, with Binder's cumulant crossing points at the last two iteration steps for the three different fractal structures: 4.217 029(41), 3.998 943(35), and 2.350 911(39). The values of $\phi_L(T_c)$, $\chi_L(T_c)$, $m_L(T_c)$, $C_L(T_c)$, and Binder's cumulant $U_L(T_c)=1-\langle M_L^4\rangle_T/3\langle M_L^2\rangle_T^2$ are reported in Table II. Once more, the exponents ν^{-1}, γ/ν, and β/ν are obtained by measuring the slopes in log-log plots. The agree-

TABLE II. The values of $\phi_L(T_c)$, $\chi_L(T_c)$, $m_L(T_c)$, $C_L(T_c)$, and $U_L(T_c)$ for the Sierpínski sponges SP(3^3,26), SP(4^3,56), and SP(3^3,18). The values of T_c are 4.217 01, 3.998 93, and 2.350 90, respectively. The values of ν^{-1}, γ/ν, and β/ν are listed in the last column.

Fractal SP		$k=1$	$k=2$	$k=3$	$k=4$	$k=5$	$\nu^{-1},\gamma/\nu,\beta/\nu$
(3^3,26)	ϕ_L	7.85(1)	51.3(2)	286.7(1.7)	1526(24)	7973(262)	$\nu^{-1}=1.505(44)$
	χ_L	0.4520(4)	4.56(2)	40.82(11)	348.2(2.5)	2942(39)	$\gamma/\nu=1.943(19)$
	m_L	0.6211(4)	0.3873(7)	0.2281(6)	0.1318(8)	0.0756(5)	$\beta/\nu=0.506(12)$
	C_L	0.8221(6)	1.527(9)	2.16(2)	2.77(5)	3.4(1)	—
	U_L	0.5209(3)	0.5109(9)	0.5107(11)	0.5132(22)	0.5149(31)	—
(4^3,56)	ϕ_L	11.35(2)	98.42(61)	721.2(9.5)	5167(161)	—	$\nu^{-1}=1.420(32)$
	χ_L	0.806(2)	13.07(5)	184.5(1.3)	2622(28)	—	$\gamma/\nu=1.914(13)$
	m_L	0.5909(5)	0.3271(6)	0.1699(4)	0.0858(4)	—	$\beta/\nu=0.493(5)$
	C_L	1.045(2)	1.818(9)	2.38(3)	2.83(9)	—	—
	U_L	0.5366(4)	0.5377(8)	0.5456(11)	0.5464(19)	—	—
(3^3,18)	ϕ_L	1.975(4)	8.85(3)	33.69(22)	122.80(65)	451.2(5.6)	$\nu^{-1}=1.185(16)$
	χ_L	0.3585(9)	2.87(1)	22.63(16)	187(1)	1674(18)	$\gamma/\nu=1.995(15)$
	m_L	0.8538(4)	0.6843(2)	0.5019(3)	0.3577(2)	0.2510(3)	$\beta/\nu=0.3224(14)$
	C_L	0.750(2)	1.355(4)	1.741(7)	1.980(6)	2.12(2)	—
	U_L	0.6219(2)	0.6287(1)	0.6345(2)	0.6374(1)	0.6375(3)	—

ment of the values of ν^{-1} and γ/ν with the values in Table I confirms the estimated critical temperature. Moreover, the consistency of the whole set of results shows that the finite-size scaling analysis works. The effective dimensions $2\beta/\nu+\gamma/\nu$, calculated from the results summarized in Table II, for the three fractals SP(3^3,26), SP(4^3,56), and SP(3^3,18), are 2.955(43), 2.900(23), and 2.640(18), respectively; the associated Hausdorff fractal dimensions $d_f=\ln N_{occ}/\ln l$ are 2.966, 2.904, and 2.631. No discrepancies between the effective dimensions and the Hausdorff ones can be brought out of our studies. It has been shown to work in fractal dimensions between 1 and 2.[7,8] This is a natural and direct consequence of the homogeneity hypothesis which states that near T_c, the free energy per spin of a finite system under the change of length scale from 1 to b with b equal to some power of l behaves as $f(t,h,L)=b^{-d_f}f(tb^{y_t},hb^{y_h},L/b)$ where $t=(T-T_c)/T_c$ and h is the external magnetic field. The Hausdorff dimension d_f appears in the above relation because, due to the self-similar character of fractal lattices, the total number of spins decreases by a factor b^{d_f} under this change. This was pointed out by Gefen *et al.*[12] in 1982 in a study of percolation clusters. Furthermore, we can estimate the exponents α/ν from the scaling law $d_f=2/\nu-\alpha/\nu$. The results calculated from Table II are $0.044(88), -0.064(64)$, and $-0.261(32)$, respectively. Numerical results show that the behavior of $C_L(T_c)$ does not follow a power law as a function of L, as previously noticed in the case of the maximum values of the specific heat. Nevertheless, the successful prediction of the critical temperature from the positions of the specific heat peaks tells us that $C_L(T)$ is dominated in the critical region by a scaling function under the form $C_L(T)=A(T)+L^{\alpha/\nu}T\mathcal{C}(tL^{1/\nu})$ where $A(T)$ is a slow variation hump function. The deviation from power laws observed in the finite-size behavior of the specific heat is obviously due to a nonzero value of $A(T)$. We are thus not able to calculate directly α/ν in a reliable way from a three-parameter fit of $C_L(T_c)$ since only four or five different sizes can be investigated and the first iteration step should be disregarded.

Scaling corrections are observed to be weaker in our case than between $d=1$ and $d=2$.[7,8] It can be related to the convergence speed of the deviation ratio $\rho(l^d,N_{occ},k)$ which is defined as the percentage of the difference between the mean number of bonds per spin at step k, called $Z(l^d,N_{occ},k)$, and that at infinite step. One can show that

$$Z(l^d,N_{occ},k)=\frac{N_I}{N_{occ}}\left[\frac{1-(N_S/N_{occ})^k}{1-(N_S/N_{occ})}\right]+\left(\frac{N_S}{N_{occ}}\right)^k d \quad (2)$$

and hence

$$\rho(l^d,N_{occ},k)=\left[\frac{(N_{occ}-N_S)d}{N_I}-1\right]\left(\frac{N_S}{N_{occ}}\right)^k, \quad (3)$$

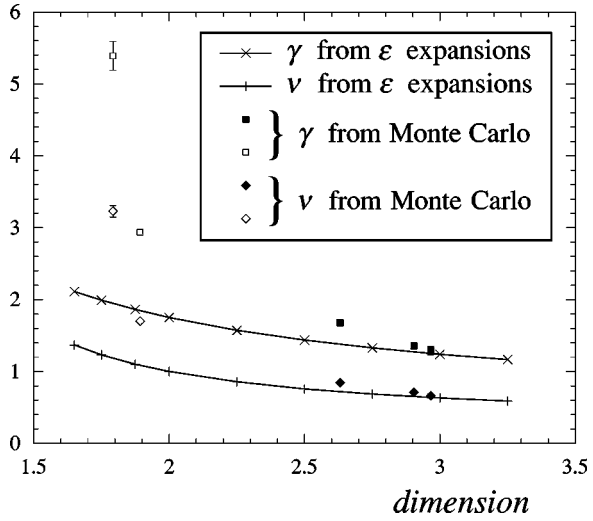

FIG. 2. Exponents γ and ν as a function of the dimension. The values of the ϵ expansion are taken from Table III of Ref. 13. The open symbols represent the values obtained by Carmona *et al.* (Ref. 8), and the solid ones the values calculated in the present work.

where N_S is the number of occupied sites on each surface of the generating cell and N_I the number of its internal bonds. As k increases, $\rho(l^d, N_{occ}, k)$ tends to zero faster than in the case of fractals embedded in a two-dimensionnal space.

We are now able to compare the exponent values obtained by Monte Carlo simulations with the values calculated by ϵ expansion for the Ising model on hypercubic lattices.[13] The obtained values of ν and γ increase as the fractal dimension decreases. This behavior is qualitatively in agreement with ϵ expansions but is not quantitatively consistent with them (see Fig. 2). The difference is due to the lack of translation symmetry of fractals. Similar situations are observed for the exponent β for either γ/ν and β/ν. Furthemore, it can be easily seen from Fig. 2 that the discrepancies between the exponents provided by the two methods are more important when the fractal dimensions are smaller than 2. Our results reinforce the suggestion of Carmona *et al.*[8] in the case of fractal dimensions below 2. These results give us enough evidence to answer the question asked by Holovatch and Yavors'kii,[14] and already pointed out by Gefen *et al.*[1] in 1980 and by Wu and Hu[15] in 1987: Does strong universality hold in the case of self-similar structures? In other words, are the critical properties only dependent upon the symmetry of the order parameter, the interaction range, and the fractal dimension? The answer is no and, in fact, it should take into account the detailed topology of the fractal lattice.

P.Y.H. thanks the ICSC World Laboratory in Switzerland for financial support. A part of numerical simulations has been carried out in the national center of computational resources IDRIS, supported by the CNRS (Project No. 991186). We acknowledge the scientific committee and the staff of the center.

[1] Y. Gefen, B.B. Mandelbrot, and A. Aharony, Phys. Rev. Lett. **45**, 855 (1980).
[2] Y. Gefen, A. Aharony, and B.B. Mandelbrot, J. Phys. A **16**, 1267 (1983).
[3] Y. Gefen, A. Aharony, Y. Shapir, and B.B. Mandelbrot, J. Phys. A **17**, 435 (1984).
[4] Y. Gefen, A. Aharony, and B.B. Mandelbrot, J. Phys. A **17**, 1277 (1984).
[5] G. Bhanot, H. Neuberger, and J.A. Shapiro, Phys. Rev. Lett. **24**, 2277 (1984).
[6] G. Bhanot, D. Duke, and R. Salvador, Phys. Lett. **165B**, 355 (1985).
[7] P. Monceau and M. Perreau, Phys. Rev. B **58**, 6386 (1998).
[8] J.M. Carmona, U.M.B. Marconi, J.J. Ruiz-Lorenzo, and A. Tarancon, Phys. Rev. B **58**, 14 387 (1998).
[9] M.E. Fisher and M.N. Barber, Phys. Rev. Lett. **28**, 1516 (1972).
[10] U. Wolff, Phys. Rev. Lett. **60**, 1461 (1988).
[11] M.N. Barber, *Phase Transitions and Critical Phenomena* (Academic, New York, 1983), Vol. 8, p. 143.
[12] Y. Gefen, A. Aharony, Y. Shapir, and A.N. Berker, J. Phys. C **15**, L801 (1982).
[13] J.C. Le Guillou and J. Zinn-Justin, J. Phys. (Paris) **48**, 19 (1987).
[14] Y. Holovatch and T. Yavors'kii, J. Stat. Phys. **92**, 785 (1998).
[15] Y.K. Wu and B. Hu, Phys. Rev. A **35**, 1404 (1987).